Chapter 7

# Thermal Conductivity of Sediment Recovered from the IMAGES VIII/PAGE 127 Gas Hydrate and Paleoclimate Cruise on the RV Marion Dufresne in the Gulf of Mexico, 2–18 July 2002

Ivana Novosel[1,2], William J. Winters[3], Olya M. Boldina[4], Cinthia Labails[5], and Louis Géli[5]

*Thermal conductivity of sediment recovered from the IMAGES VIII/PAGE 127 gas hydrate and paleoclimate cruise on the RV* Marion Dufresne *in the Gulf of Mexico, 2–18 July 2002; chapter 7* in *Winters, W.J., Lorenson, T.D., and Paull, C.K., eds., 2007, Initial report of the IMAGES VIII/PAGE 127 gas hydrate and paleoclimate cruise on the RV* Marion Dufresne *in the Gulf of Mexico, 2–18 July 2002: U.S. Geological Survey Open-File Report 2004–1358.*

## Introduction

A scientific piston-coring cruise aimed at studying the distribution of shallow gas hydrate deposits was conducted aboard the RV *Marion Dufresne* in July 2002. Thermal conductivity, a property related to the rate of heat transport through a medium and used to determine heat flow, was measured on a total of 23 cores. Ten cores were from Tunica Mound, four were from Bush Hill, and nine were from the Mississippi Canyon area. Only one core containing gas hydrate, MD02-2565, from the Mississippi Canyon 853 diapir was tested for thermal conductivity. Core information, including water depth, is presented in Appendix A, and maps of core locations are in Appendix B of this report.

## Methods

When a core became accessible on the ship's deck, it was labeled and cut into 1.5-meter (m)-long sections for ease in handling (Winters and others, this volume, chapter 3). The sections then were brought into thermal equilibrium with ambient temperature in the laboratory in preparation for thermal conductivity measurements. In this study, two separate instruments using the pulsed-needle probe transient method (Lister, 1979) were used to determine thermal conductivities. The system used for the first half of the cruise was provided by T. Lewis (Geological Survey of Canada – Pacific Geoscience Center, GSC–PGC), and a more automated 'black-box' type system provided by L. Geli (French Research Institute for Exploitation of the Sea, IFRAMER) was used for the second half of the cruise. It is believed that the change in equipment had minimal, if any, effect on results because both systems produced nearly identical data during a transition period when multiple tests were performed on the same sediment.

The measuring equipment consisted of (1) an ~2-millimeter (mm) diameter and 70-mm-long needle probe with a constant calibration resistance of 40.3 ohm, (2) a programmable power supply producing 2.6 joules of total energy per 10-mm length of probe, (3) a multi-meter that measured the resistance of the thermistor every 0.5 second(s), and (4) a computer for logging and calculations. Each system had one needle probe, and each probe was calibrated once using food-grade clear gelatin, which was assumed to have thermal conductivity properties similar to water. Measurements were repeated occasionally to check for variability. The uncertainty range for the measurements is less than 10 percent.

[1]University of Victoria, School of Earth and Ocean Sciences, Victoria, BC, V8W 3P6 Canada.

[2]Currently at: Rice University, Department of Earth Science, 6100 Main Street, Houston, TX 77005 USA.

[3]U.S. Geological Survey, 384 Woods Hole Road, Woods Hole, MA 02543 USA.

[4]Moscow State University, Department of Geocryology, Moscow, Russia 119992.

[5]Marine Geosciences Department, IFRAMER, BP 70, 29280, Plouzané, France.

The change in the temperature inside a probe can be described by the following relation (Lewis and others, 1993):

$$T(t)=Q/(4\pi\kappa t),$$

where

- $Q$ is the total heat input per unit length of the probe;
- $\kappa$ is the thermal conductivity;
- $t$ is the time since the start of the heat pulse; and
- $T$ is the temperature change, in degrees Kelvin.

The thermal conductivity is obtained by defining the slope of the temperature decay curve on a T versus 1/t graph.

Thermal conductivities were measured approximately once per standard 1.5-m core section. A small hole was hand-drilled (to avoid excessive heat generation) into the core liner through which the needle probe was immediately inserted. For the first system, the temperature drift was measured, and a heat pulse was applied only if the drift was less than 0.0003 degrees Kelvin per second (K/s). The decay of temperature with time was measured and displayed on a graph to check the quality of the data and to visually choose the proper time window based on test duration and system response for the determination of the conductivity. In this study, the window was commonly set to 30 to 70 s after the heat pulse. These steps were omitted while using the second, more automated system.

## Results

Thermal conductivities of all core samples (table 1) range from 0.00 (in the presence of gas) to 2.64 W/m•K (watt per meter times degrees Kelvin) with a mean of 0.93 W/m•K and a median of 0.95 W/m•K (table 2). Values were plotted with subbottom depth for the three different study areas—Tunica Mound (fig. 1), Bush Hill (fig. 2), and Mississippi Canyon region (figs. 3, 4). Thermal conductivity values typically increase with depth from approximately 0.8 to 1.0 W/m•K, with a greater rate of increase within the top 10 to 15 m of sediment than deeper in the core.

## Conclusions

Thermal conductivity increases more rapidly in the upper 10 to 15 m of sediment than below that depth where values decrease at a more gradual rate or are nearly constant with depth. This change in behavior coincides with water content and porosity trends noted in Winters and others (this volume, chapter 4). This is reasonable considering the relation between thermal conductivity and water content. Thermal conductivity in sediments collected offshore Vancouver Island on the Cascadia accretionary prism also changed more abruptly in shallow subbottom sediment (Novosel, 2002).

Except for a few outlying points, the thermal conductivities presented for Tunica Mound (fig. 1) and Bush Hill (fig. 2) have much less scatter in relation to depth than at the Mississippi Canyon region (fig. 4), where almost all the low values are present in only two cores—MD02-2565 and MD02-2570. If results are plotted without data from those two cores, the scatter is equivalent to or better than at Tunica Mound and Bush Hill (fig. 5). The upper linear trend of thermal conductivity in relation to depth of the Mississippi Canyon sediment as shown in figure 5 extends to about 15 meters below sea floor (mbsf), deeper than at either Tunica Mound or Bush Hill.

Because gas hydrate was recovered in core MD02-2565, the likely cause of the low thermal conductivities is the presence of free gas caused by hydrate dissociation. Similar gas expansion effects on thermal conductivity values of shallow gas hydrate-bearing sediments is also observed on the Cascadia margin (Novosel, 2002; Riedel and others, 2005). Thermal conductivities are also low in core MD02-2570, suggesting free gas may have been present in that core as well. This interpretation is supported by core photographs showing numerous expansion cracks in core MD02-2570 (Appendix G). These cracks were not observable during thermal conductivity

**Table 1.** Summary of thermal conductivity measurements.

[Note: Core MD02-2548 is not a USGS core. Thermal conductivitiy values (W/m•K) for core MD02-2548 are presented in this table for information purposes only. The values for core MD02-2548 are not plotted in figure 1]

| Depth (cm) | Thermal Conductivity (W/m•K) | Depth (cm) | Thermal Conductivity (W/m•K) | Depth (cm) | Thermal Conductivity (W/m•K) | Depth (cm) | Thermal Conductivity (W/m•K) | Depth (cm) | Thermal Conductivity (W/m•K) |
|---|---|---|---|---|---|---|---|---|---|
| **MD022535** | | 220 | 0.83 | 850 | 0.83 | 680 | 0.85 | 2770 | 0.98 |
| 70 | 0.82 | 370 | 0.85 | 915 | 0.86 | 825 | 0.92 | 2920 | 0.88 |
| 90 | 0.85 | 520 | 0.92 | **MD022546** | | 925 | 0.95 | 3070 | 1.06 |
| 220 | 0.79 | 670 | 1.00 | 70 | 0.81 | 1115 | 0.92 | 3210 | 1.02 |
| 380 | 0.92 | 820 | 1.06 | 220 | 0.73 | 1265 | 0.90 | 3370 | 1.01 |
| 520 | 0.95 | 970 | 1.13 | 370 | 0.88 | 1415 | 0.33 | **MD022557** | |
| 680 | 1.02 | 1120 | 1.10 | 520 | 0.91 | 1565 | 1.01 | 70 | 0.85 |
| 830 | 1.06 | 1270 | 1.03 | 670 | 0.98 | 1725 | 1.08 | 220 | 0.86 |
| 980 | 1.05 | 1420 | 1.06 | 780 | 0.94 | 1830 | 0.90 | 375 | 1.02 |
| 1110 | 1.11 | 1570 | 1.07 | 860 | 0.97 | 2000 | 0.88 | 510 | 1.04 |
| 1270 | 1.09 | 1720 | 1.06 | 970 | 0.94 | 2145 | 0.79 | **MD022559** | |
| 1420 | 1.02 | 1870 | 0.98 | 1110 | 0.92 | 2300 | 1.00 | 60 | 0.83 |
| 1570 | 1.04 | 2020 | 1.03 | 1280 | 0.99 | 2450 | 1.06 | 220 | 0.84 |
| 1720 | 0.98 | 2170 | 0.99 | 1410 | 0.79 | 2595 | 1.08 | 370 | 0.81 |
| 1880 | 1.07 | 2320 | 0.95 | 1570 | 0.90 | 2745 | 1.07 | 520 | 0.88 |
| 2000 | 0.97 | 2470 | 1.07 | 1720 | 0.95 | 2895 | 0.96 | 660 | 0.79 |
| 2160 | 0.94 | 2620 | 0.97 | 1870 | 0.73 | 3030 | 1.02 | 820 | 0.91 |
| 2320 | 0.98 | 2770 | 0.97 | 1960 | 0.90 | **MD022555** | | 970 | 0.90 |
| 2480 | 1.02 | 2920 | 1.08 | 2040 | 0.97 | 70 | 0.80 | 1120 | 0.96 |
| 2620 | 0.99 | 3070 | 0.99 | 2170 | 0.94 | 185 | 0.84 | 1260 | 0.96 |
| 2760 | 1.00 | MD022541 | | 2320 | 0.95 | 370 | 0.86 | 1420 | 1.08 |
| 2920 | 0.99 | 60 | 0.88 | 2450 | 0.94 | 520 | 0.90 | 1570 | 0.95 |
| 3060 | 0.99 | 220 | 0.90 | 2620 | 0.99 | 670 | 0.87 | 1720 | 1.07 |
| 3220 | 1.02 | 370 | 0.91 | 2770 | 0.98 | 820 | 0.91 | 1870 | 0.99 |
| 3360 | 1.00 | 520 | 0.91 | 2920 | 0.92 | 970 | 1.00 | 2010 | 1.03 |
| 3500 | 1.01 | 670 | 1.00 | 3060 | 0.97 | 1120 | 0.96 | 2170 | 1.13 |
| 3640 | 0.98 | 820 | 1.07 | **MD022547** | | 1260 | 0.96 | 2320 | 1.18 |
| 3760 | 0.96 | 970 | 1.04 | 75 | 0.81 | 1420 | 0.87 | 2470 | 1.12 |
| MD022537 | | 1120 | 1.23 | 220 | 0.85 | 1680 | 1.02 | 2620 | 1.01 |
| 75 | 0.84 | 1270 | 1.14 | 370 | 0.90 | 1720 | 1.02 | 2770 | 1.16 |
| 225 | 0.85 | 1420 | 1.02 | 510 | 0.90 | 1870 | 1.09 | 2910 | 1.25 |
| 375 | 0.92 | 1570 | 0.97 | **MD022548** | | 2020 | 1.03 | 3070 | 1.29 |
| 520 | 0.92 | 1720 | 1.01 | 80 | 0.82 | 2160 | 1.00 | 3210 | 1.16 |
| 675 | 0.92 | 1870 | 0.99 | 220 | 0.84 | 2320 | 1.06 | 3320 | 1.22 |
| 820 | 0.97 | 2020 | 1.13 | 370 | 0.88 | 2480 | 1.15 | **MD022560** | |
| 980 | 1.05 | 2170 | 0.96 | 520 | 0.86 | 2620 | 1.06 | 60 | 0.49 |
| 1120 | 1.00 | 2320 | 0.98 | 680 | 0.99 | 2770 | 1.10 | 220 | 0.90 |
| 1275 | 0.98 | 2470 | 0.96 | 780 | 0.94 | 2920 | 1.03 | 370 | 0.82 |
| 1420 | 1.00 | 2620 | 0.99 | 940 | 1.02 | 3070 | 0.90 | 520 | 0.91 |
| 1580 | 0.95 | 2770 | 0.95 | 1020 | 0.98 | 3220 | 0.99 | 655 | 0.84 |
| 1710 | 0.92 | 2920 | 0.97 | 1130 | 0.98 | 3380 | 1.06 | 820 | 0.93 |
| 1870 | 1.00 | 3070 | 0.99 | 1280 | 1.03 | 3510 | 1.08 | 970 | 0.93 |
| 2020 | 0.96 | 3220 | 0.97 | 1420 | 0.93 | **MD022556** | | 1115 | 0.99 |
| 2170 | 0.98 | 3370 | 0.99 | 1570 | 0.99 | 70 | 0.86 | 1262 | 1.01 |
| 2320 | 0.95 | 3570 | 1.19 | 1730 | 0.95 | 220 | 0.90 | 1420 | 1.02 |
| 2475 | 0.95 | **MD022542** | | 1880 | 1.07 | 380 | 0.83 | 1570 | 1.00 |
| 2620 | 0.97 | 80 | 0.84 | 1960 | 0.90 | 520 | 0.83 | 1725 | 0.99 |
| 2770 | 0.96 | 220 | 0.83 | 2030 | 0.94 | 670 | 0.89 | 1870 | 0.96 |
| 2895 | 0.91 | 370 | 0.95 | 2180 | 0.95 | 810 | 1.12 | 2010 | 1.09 |
| 3005 | 0.96 | 530 | 1.05 | 2330 | 0.99 | 970 | 0.98 | 2180 | 0.96 |
| 3165 | 0.87 | 680 | 0.97 | 2470 | 1.01 | 1160 | 0.96 | 2320 | 0.93 |
| 3310 | 0.96 | 760 | 1.02 | 2620 | 1.00 | 1270 | 0.82 | 2470 | 1.03 |
| MD022538 | | **MD022545** | | 2780 | 1.02 | 1420 | 0.99 | 2610 | 0.99 |
| 70 | 0.85 | 40 | 0.84 | 2925 | 0.95 | 1540 | 1.00 | 2760 | 1.08 |
| 220 | 0.85 | 145 | 0.81 | 3075 | 1.00 | 1720 | 0.99 | **MD022561** | |
| 370 | 0.91 | 250 | 0.85 | 3220 | 1.00 | 1870 | 0.95 | 70 | 0.73 |
| 570 | 0.96 | 345 | 1.02 | **MD022554** | | 2020 | 0.99 | 200 | 0.87 |
| 670 | 0.95 | 445 | 0.47 | 70 | 0.76 | 2170 | 0.98 | 370 | 0.80 |
| 765 | 0.95 | 545 | 0.54 | 220 | 0.85 | 2340 | 1.03 | 520 | 0.84 |
| MD022539 | | 650 | 0.88 | 370 | 0.87 | 2480 | 1.05 | 660 | 0.88 |
| 60 | 0.82 | 740 | 0.91 | 520 | 0.86 | 2620 | 1.08 | 820 | 0.96 |

**Table 1.** Summary of thermal conductivity measurements. — Continued

[Note: Core MD02-2548 is not a USGS core. Thermal conductivitiy values (W/m•K) for core MD02-2548 are presented in this table for information purposes only. The values for core MD02-2548 are not plotted in figure 1]

| Depth (cm) | Thermal Conductivity (W/m•K) | Depth (cm) | Thermal Conductivity (W/m•K) | Depth (cm) | Thermal Conductivity (W/m•K) | Depth (cm) | Thermal Conductivity (W/m•K) | Depth (cm) | Thermal Conductivity (W/m•K) |
|---|---|---|---|---|---|---|---|---|---|
| 970 | 0.90 | 480 | 0.03 | 565 | 0.86 | 485 | 0.77 | 240 | 0.86 |
| 1090 | 1.00 | 530 | 0.66 | 625 | 0.93 | 520 | 0.92 | 320 | 0.85 |
| 1270 | 1.01 | 625 | 0.75 | 660 | 0.95 | 565 | 0.87 | 370 | 0.83 |
| 1420 | 1.08 | 675 | 0.75 | 775 | 0.87 | 620 | 0.93 | 420 | 0.25 |
| 1570 | 1.03 | 725 | 0.75 | 820 | 0.93 | 660 | 0.90 | 470 | 0.81 |
| 1730 | 1.04 | 775 | 0.69 | 865 | 0.92 | 775 | 0.96 | 510 | 0.82 |
| 1870 | 1.05 | 810 | 0.60 | 925 | 1.93 | 820 | 0.97 | 550 | 0.77 |
| 2020 | 1.09 | 850 | 0.65 | 970 | 0.96 | 865 | 0.84 | 620 | 0.84 |
| 2170 | 0.98 | 925 | 0.72 | 1015 | 0.94 | 920 | 0.90 | 650 | 0.80 |
| 2330 | 1.16 | 985 | 0.66 | 1145 | 1.05 | 970 | 0.96 | 690 | 0.91 |
| 2470 | 1.13 | 1075 | 0.81 | 1080 | 0.88 | 1020 | 1.64 | 780 | 0.84 |
| 2620 | 1.12 | 1120 | 0.71 | 1220 | 0.93 | 1070 | 0.98 | 820 | 0.85 |
| 2760 | 1.00 | 1160 | 0.72 | 1255 | 1.07 | 1130 | 1.06 | 860 | 0.83 |
| 2870 | 0.32 | 1310 | 0.76 | 1290 | 1.00 | 1225 | 0.92 | 980 | 0.74 |
| **MD022562** | | 1225 | 0.70 | 1375 | 1.03 | 1290 | 1.01 | 1020 | 0.81 |
| 60 | 0.87 | 1270 | 0.77 | 1420 | 1.04 | 1370 | 0.97 | 1080 | 0.86 |
| 205 | 0.90 | 1450 | 0.77 | 1465 | 0.92 | 1420 | 0.90 | 1140 | 0.88 |
| 370 | 0.86 | 1410 | 0.71 | 1525 | 1.04 | 1465 | 1.06 | 1260 | 0.98 |
| 520 | 0.93 | 1370 | 0.77 | 1570 | 1.02 | 1520 | 1.08 | 1320 | 0.84 |
| 640 | 0.99 | 1520 | 0.83 | 1615 | 0.99 | 1570 | 1.04 | 1380 | 0.87 |
| 820 | 0.97 | 1570 | 0.62 | 1665 | 0.90 | 1620 | 1.09 | 1420 | 0.63 |
| 970 | 1.10 | 1610 | 0.71 | 1720 | 1.03 | 1670 | 1.01 | 1460 | 0.84 |
| 1110 | 1.06 | 1670 | 0.72 | 1765 | 1.08 | 1720 | 1.13 | 1540 | 0.76 |
| 1260 | 1.08 | 1700 | 0.76 | 1820 | 0.93 | 1770 | 1.07 | 1580 | 0.80 |
| 1420 | 1.12 | 1760 | 0.73 | 1855 | 1.19 | 1825 | 1.09 | 1620 | 0.71 |
| 1560 | 1.05 | 1680 | 0.80 | 1890 | 0.00 | 1890 | 1.13 | 1680 | 0.81 |
| 1720 | 1.13 | 1840 | 0.73 | 1975 | 1.13 | 1970 | 1.09 | 1740 | 0.81 |
| 1860 | 1.13 | 1880 | 0.81 | 2020 | 1.11 | 2020 | 1.07 | 1820 | 0.82 |
| 2035 | 1.15 | 1980 | 0.65 | 2065 | 1.07 | 2070 | 1.08 | 1880 | 0.66 |
| 2170 | 1.01 | 2020 | 0.77 | 2125 | 0.99 | 2120 | 1.18 | 1920 | 0.67 |
| 2320 | 1.11 | 2060 | 0.71 | 2170 | 1.16 | 2170 | 1.00 | 1980 | 0.70 |
| 2460 | 1.07 | 2120 | 0.67 | 2215 | 1.09 | 2220 | 1.12 | 2020 | 0.69 |
| 2580 | 1.00 | 2170 | 0.73 | 2275 | 1.05 | 2275 | 1.11 | 2060 | 0.87 |
| **MD022564** | | 2215 | 0.83 | 2320 | 1.11 | 2320 | 1.18 | 2120 | 0.86 |
| 80 | 0.83 | 2280 | 0.63 | 2365 | 0.00 | 2365 | 1.03 | 2180 | 0.84 |
| 220 | 0.81 | 2320 | 0.75 | 2430 | 1.02 | 2420 | 1.04 | 2210 | 0.79 |
| 370 | 0.87 | **MD022566** | | 2480 | 1.04 | 2455 | 1.09 | 2260 | 0.76 |
| 530 | 0.91 | 20 | 0.82 | 2580 | 1.06 | 2490 | 1.00 | 2340 | 0.69 |
| 670 | 0.99 | 60 | 0.80 | **MD022567** | | 2570 | 0.93 | 2420 | 0.83 |
| 755 | 0.95 | 90 | 0.78 | 20 | 0.78 | 2605 | 1.00 | 2490 | 0.77 |
| **MD022565** | | 235 | 0.86 | 60 | 0.85 | 2640 | 1.00 | 2510 | 0.78 |
| 40 | 0.67 | 175 | 0.78 | 90 | 0.88 | **MD022570** | | 2570 | 0.93 |
| 85 | 2.64 | 325 | 0.81 | 175 | 0.85 | 20 | 0.49 | 2620 | 0.75 |
| 180 | 0.69 | 370 | 0.80 | 225 | 0.83 | 55 | 0.90 | 2670 | 0.87 |
| 220 | 0.73 | 415 | 0.86 | 325 | 0.79 | 90 | 0.88 | 2720 | 0.83 |
| 260 | 0.69 | 475 | 0.84 | 380 | 0.83 | 170 | 0.87 | 2760 | 0.91 |
| 340 | 0.72 | 520 | 0.84 | 420 | 0.90 | 205 | 0.89 | 2810 | 0.67 |

**Table 2.** Statistical values for the thermal conductivity (W/m•K) measurements.

| | Tunica Mound | Bush Hill | Mississippi Canyon region | Mississippi Canyon region without MD02-2565 and MD02-2570 | All regions |
|---|---|---|---|---|---|
| Minimum | 0.47 | 0.33 | 0 | 0 | 0 |
| Maximum | 1.23 | 1.15 | 2.64 | 1.93 | 2.64 |
| Range | 0.76 | 0.82 | 2.64 | 1.93 | 2.64 |
| Mean | 0.95 | 0.95 | 0.91 | 0.97 | 0.93 |
| Median | 0.97 | 0.98 | 0.9 | 0.99 | 0.95 |
| Standard deviation | 0.10 | 0.12 | 0.22 | 0.18 | 0.18 |

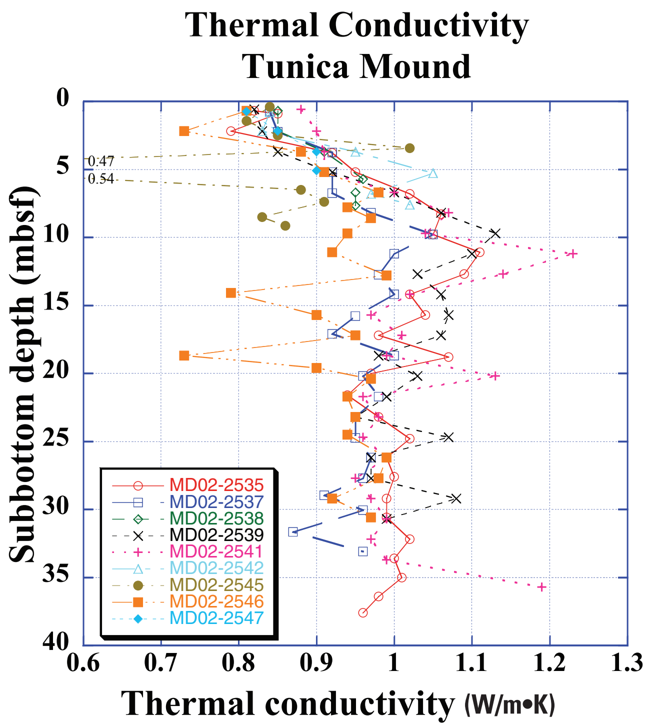


**Figure 1.** Thermal conductivity values (0.6 to 1.3 W/m•K) in relation to subbottom depth for Tunica Mound.

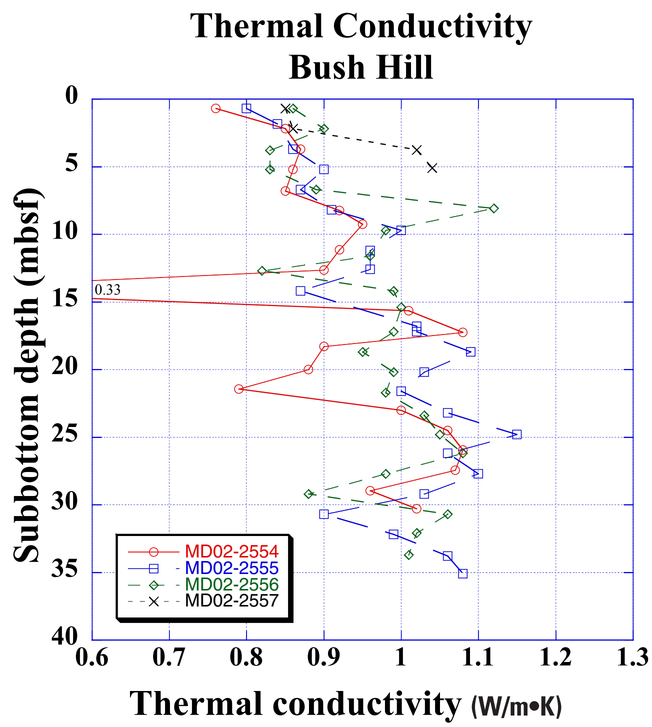


**Figure 2.** Thermal conductivity values (0.6 to 1.3 W/m•K) in relation to subbottom depth for Bush Hill.

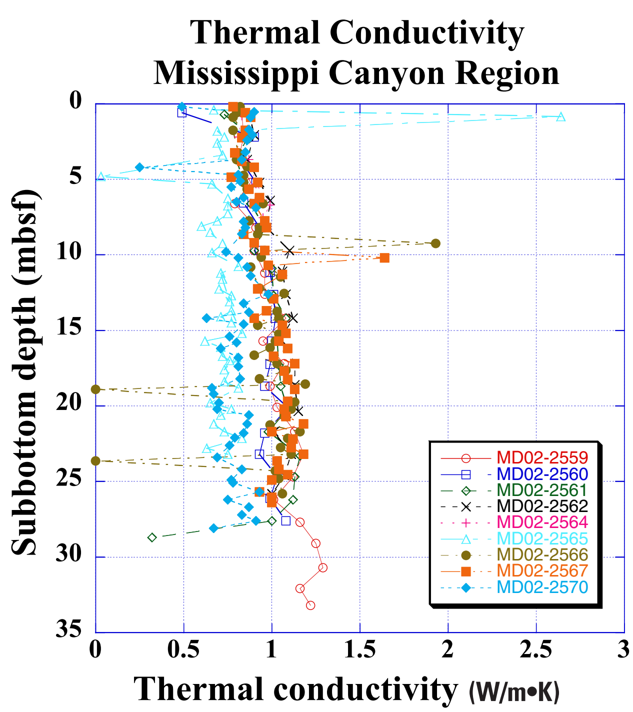


**Figure 3.** Thermal conductivity values (0 to 3 W/m•K) in relation to subbottom depth for the Mississippi Canyon region.

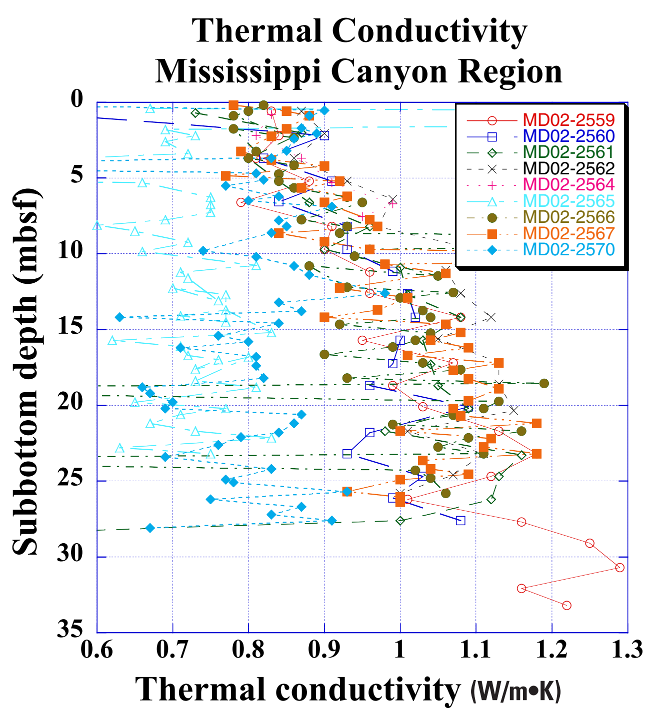


**Figure 4.** Thermal conductivity values (0.6 to 1.3 W/m•K) in relation to subbottom depth for the Mississippi Canyon region.

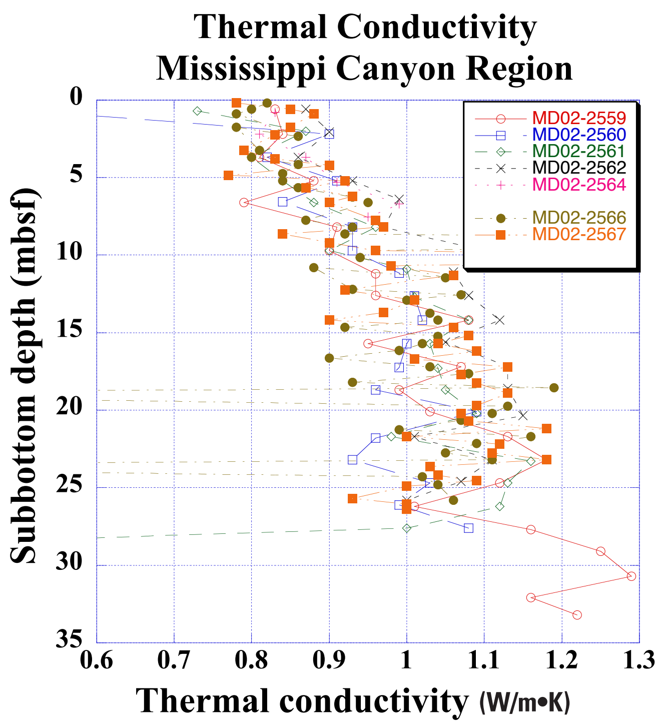


**Figure 5.** Thermal conductivity values (0.6 to 1.3 W/m•K) without data from cores MD02-2565 and MD02-2570 in relation to subbottom depth for the Mississippi Canyon region.

measurements (because of the opaque core liner) and were discovered subsequently when the cores were split for conducting additional physical property analyses.

## References Cited


Lewis, T.J., Villinger, H., and Davis, E.E., 1993, Thermal conductivity measurement of rock fragments using a pulsed needle probe: Canadian Journal of Earth Sciences, v. 30, no. 3, p. 480–485.

Lister, C.R.B., 1979, The pulse-probe method of conductivity measurement: Geophysical Journal, v. 57, p. 451–461.

Novosel, I., 2002, Physical properties of gas hydrate related sediments offshore Vancouver Island, M.S. Thesis, University of Victoria, Canada.

Riedel, M., Novosel, I., Spence, G.D., Hyndman, R.D., Chapman, R.N., Solem, R.C., and Lewis, T., in press, Geophysical and geochemical signatures associated with gas hydrate related venting at the North Cascadia Margin: Geological Society of America Bulletin.